VOLUME 113, NUMBER 7
MARCH 27, 1991

JOURNAL OF THE AMERICAN CHEMICAL SOCIETY

Multinuclear ENDOR Study of Trapped Electrons in the Polycrystalline Sodide $Cs^+(HMHCY)\cdot Na^-$

Ahmed S. Ellaboudy, Christopher J. Bender, Jineun Kim, Dae-Ho Shin, Mark E. Kuchenmeister, Gerald T. Babcock, and James L. Dye*

Contribution from the Department of Chemistry and Center for Fundamental Materials Research, Michigan State University, East Lansing, Michigan 48824. *Received August 15, 1990*

Abstract: Synthesis of the sodide $Cs^+(HMHCY)\cdot Na^-$, in which HMHCY is the cation complexant hexamethylhexacyclen [Kuchenmeister, M. E.; Dye, J. L. *J. Am. Chem. Soc.* **1989**, *111*, 935], always leads to the inclusion of trapped electrons. The nature of the trapping site has been explored by EPR and multinuclear ENDOR techniques. Pronounced axial hyperfine coupling to a single cesium nucleus is in accord with an F-center model in which Na^- vacancies are occupied by trapped electrons. Dipolar and contact coupling to $-CH_3$ protons as measured by ^1H ENDOR studies of the protio- and deuteriomethyl compounds is also in accord with this model. ENDOR signals from ^{23}Na and ^{133}Cs reflect the NMR powder patterns of these nuclei and correspond to small Fermi contact densities (0.079 and 0.014 or 0.091 and 0.018% atomic character, respectively, depending on the choice of sign for the hyperfine coupling constant) resulting from the "tails" of the trapped electron distribution. It is suggested that electron trapping in alkalides is similar to that which occurs at all anionic sites in electrides.

Introduction

The nature of electron traps in liquids and solids has been the subject of many theoretical and experimental studies. The systems involved range from the well-understood F-centers, in which electrons are trapped at anion vacancies,[1,2] to solvated electrons in fluid media.[3-10] Although there is not universal agreement about the nature of solvated electrons, the most common view is that the electrons occupy a cavity in the solvent, a picture that has gained additional credence with the advent of molecular dynamics calculations.[11-13] Electrons can also be trapped in glasses at low temperatures and appear also to occupy cavities or solvent vacancies in these media.[14,15]

In all of the cases described above, except for concentrated metal solutions in ammonia and methylamine, the electron traps are dilute, so that electron–elecron interactions are either weak or confined to pairs or small clusters of electrons and counterions. In this situation, an important aspect of the cavity model is that the electron is not strictly confined to the cavity—rather, the electronic wave function can extend into the surroundings, leading

(1) Fowler, W. B. *Physics of Color Centers*; Academic Press: New York, 1968.
(2) Schulman, J. H.; Compton, W. D. *Color Centers in Solids*; Pergamon Press: New York, 1962.
(3) Thompson, J. C. *Electrons in Liquid Ammonia*; Oxford University Press: Oxford, 1976.
(4) Gould, R. F., Ed. *Advances in Chemistry Series 50*; American Chemical Society: Washington, DC, 1965.
(5) Lepourtre, G.; Sienko, M. J., Eds. *Metal Ammonia Solutions, Colloque Weyl I*; Benjamin: New York, 1974.
(6) Lagowksi, J. J.; Sienko, M. J., Eds. *Metal Ammonia Solutions, Colloque Weyl II*; IUPAC/Butterworths: London, 1970.
(7) Jortner, J.; Kestner, N. R., Eds. *Electrons in Fluids, Colloque Weyl III*; Springer-Verlag: Berlin, 1973.
(8) Dye, J. L., Conference Organizer. *Colloque Weyl IV. Electrons in Fluids. The Nature of Metal-Ammonia Solutions*: *J. Phys. Chem.* **1975**, *79*, 2789–3079.
(9) Webster, B., Conference Organizer. *Colloque Weyl V. The 5th Int. Conf. Excess Electrons. Metal-Ammonia Solutions*: *J. Phys. Chem.* **1980**, *84*, 1065–1298.
(10) Thompson, J. C., Conference Organizer. *Colloque Weyl VI. The 6th Int. Conf. Excess Electrons. Metal-Ammonia Solutions*: *J. Phys. Chem.* **1984**, *88*, 3699–3913.
(11) Rossky, P. J.; Schnitker, J. *J. Phys. Chem.* **1988**, *92*, 4277.
(12) Schnitker, J.; Rossky, P. J.; Kenney-Wallace, G. A. *J. Chem. Phys.* **1986**, *85*, 2986.
(13) Jonah, C. D.; Romero, C.; Rahman, A. *Chem. Phys. Lett.* **1986**, *123*, 209.
(14) Kevan, L. *Acc. Chem. Res.* **1981**, *14*, 138.
(15) Narayana, P. A.; Bowman, M. K.; Kevan, L.; Yudanov, V. F.; Tsretkov, Y. D. *J. Chem. Phys.* **1975**, *63*, 3365.

0002-7863/91/1513-2347$02.50/0

to hyperfine interactions with nearby nuclei. Thus, in the absence of strong electron–electron interactions, magnetic coupling between the trapped electrons and nearby nuclei should be observable.

Recently we have synthesized and studied a new class of compounds, crystalline *electrides*[16-24] in which stoichiometric amounts of trapped electrons serve as the "counterions" to complexed alkali-metal cations. The electronic, optical, and magnetic properties of electrides and their structural similarity to the corresponding *alkalides* (salts in which alkali-metal anions are present) strongly point to stoichiometric electron trapping at the anionic sites. The structures[19,22,23] have large vacancies at the anionic sites, but any electron density in these cavities would be far too small to have been detected by the X-ray crystallography methods used. Thus, electron-trapping at all the anionic vacancies can be inferred, but not demonstrated conclusively. Attempts to "map" the electron distribution in pure electrides by EPR and ENDOR techniques have not been successful, presumably because of rapid electron exchange.

When alkalide salts are synthesized by crystallization from a solution that contains the complexed cation $M_aC_n^+$ and the alkali-metal anion, M_b^- (where M_a and M_b may be the same or different and n is 1 or 2), electrons are invariably also present in the crystal, albeit at low concentrations (<1% typically).[24-26] The presence of trapped electrons in the crystal occurs because a solution that contains M^- also always contains some solvated electrons as a result of the dissociation equilibrium.

$$M^- \rightleftarrows M^+ + 2e^-_{solv} \qquad (1)$$

One can also increase the electron content by decreasing the amount of metal relative to the complexant. Thus, alkalides naturally contain trapped electrons that are, on the average, far enough apart to suppress electron-exchange phenomena. In the present work, we take advantage of electron localization in the very stable sodide salt $Cs^+(HMHCY)\cdot Na^-$[27,28] to examine interactions of the trapped electron with the surrounding nuclei by using ENDOR techniques.

Experimental Section

The synthesis of the title compound is similar to those of the alkalide salts previously reported.[26] Hexacyclen, the precursor to the complexant HMHCY, was purchased as the sulfate salt (Aldrich) and was methylated[29] or deuteriomethylated in the Michigan State University Synthesis Laboratory.

EPR and ENDOR spectra were recorded with an X-band ER 200D Series Bruker spectrometer equipped with an ER 250 ENDOR/triple accessory and an ER 250 ENB cavity.[30] The spectrometer is controlled by a Nicolet 1180 data system. The radio frequency power was supplied to the helical ENDOR coil from an ENI 3100L amplifier driven at frequencies generated by a Wavetek (3000-446) synthesizer. A flow cryogenic system was used for low-temperature work, while an Oxford Instruments ESR-900 cryostat was used at liquid helium temperatures.

The ENDOR coil used in the experiment was a modified version of a previously published design.[31] The coil consists of a silver wire helix with the number of turns determined by the frequency range to be covered in the experiment. Much of the brass used in the published design to make electrical contact was cut away to reduce stray capacitance. The impedance of the radio frequency circuit was matched when necessary with impedance transformers built in our laboratory following a design by Ruthroff.[32] The ENDOR cavity has a Q-factor in excess of 800 when loaded with a coil and quartz dewar insert. The g value and free nuclear resonant frequencies were determined by direct measurement of the magnetic field strength and microwave frequency with an ER 035M NMR gaussmeter and a Hewlett-Packard 5245 counter equipped with a 15255 converter which operates at 3-12 GHz.

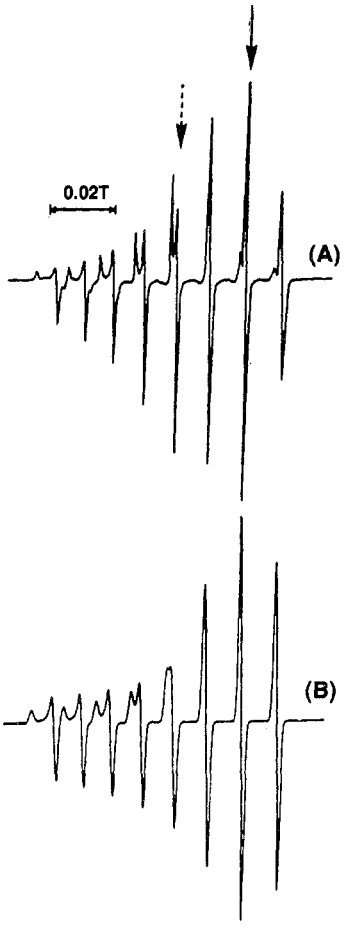

Figure 1. (A) X-band EPR spectrum of a polycrystalline sample of $Cs^+(HMHCY)\cdot Na^-$ (the arrows indicate the fields at which the ENDOR spectra were recorded); (B) computer-simulated spectrum of the major EPR signal.

Results

1. EPR Studies. The X-band spectrum of the title compound is shown in Figure 1A. The presence of a major set of octets results from hyperfine electron coupling (Fermi contact) to the cesium nucleus ($I = {}^7/_2$). The presence of another very minor set of octets with a slightly smaller coupling constant is apparent. Each hyperfine component shows a first derivative axially symmetric powder pattern that reflects the symmetry of both the g and A tensors. Power saturation studies of the deuteriomethyl compound reveal that each line is homogeneously broadened with $T_1 = 3.3 \times 10^{-4}$ s and $T_2 = 7.6 \times 10^{-9}$ s, indicating the absence of appreciable unresolved hyperfine interactions to hydrogen or sodium nuclei. The m_I dependence of both the line intensity and the separation is an indication of the anisotropy of the system.

(16) Ellaboudy, A.; Dye, J. L.; Smith, P. B. *J. Am. Chem. Soc.* **1983**, *105*, 6490.
(17) Dye, J. L.; Ellaboudy, A. *Chem. Br.* **1984**, *20*, 210.
(18) Dye, J. L. *Prog. Inorg. Chem.* **1984**, *32*, 327.
(19) Dawes, S. B.; Ward, D. L.; Huang, R. H.; Dye, J. L. *J. Am. Chem. Soc.* **1986**, *108*, 3534.
(20) Dye, J. L.; DeBacker, M. G. *Annu. Rev. Phys. Chem.* **1987**, *38*, 271.
(21) Dye, J. L. *Sci. Am.* **1987**, *257*, 66.
(22) Huang, R. H.; Faber, M. K.; Moeggenborg, K. J.; Ward, D. L.; Dye, J. L. *Nature* **1988**, *331*, 599.
(23) Ward, D. L.; Huang, R. H.; Dye, J. L. *Acta Crystallogr.* **1988**, *C44*, 1374.
(24) Dawes, S. B.; Ward, D. L.; Fussa-Rydel, O.; Huang, R. H.; Dye, J. L. *Inorg. Chem.* **1989**, *28*, 2132.
(25) Issa, D.; Ellaboudy, A.; Janakiraman, R.; Dye, J. L. *J. Phys. Chem.* **1984**, *88*, 3847.
(26) Dye, J. L. *J. Phys. Chem.* **1984**, *88*, 3842.
(27) Kuchenmeister, M. E.; Dye, J. L. *J. Am. Chem. Soc.* **1989**, *111*, 935.
(28) The abbreviation HMHCY refers to the complexant hexamethylhexacyclen: IUPAC, 1,4,7,10,13,16-hexaaza-1,4,7,10,13,16-hexamethylcyclooctadecane.
(29) Barrett, A. G. M.; Godfrey, C. R. A.; Hollinshead, D. M.; Prokopiou, P. A.; Barton, D. H. R.; Boar, R. B.; Joukhadar, L.; McGhie, J. F.; Misra, S. C. *J. Chem. Soc., Perkin Trans. I* **1981**, 1501.
(30) Bender, C. J.; Sahlin, M.; Babcock, G. T.; Barry, B. A.; Chandrashekar, T. K.; Salowe, S. P.; Stubbe, J. A.; Lindstrom, B.; Petersson, L.; Ehrenberg, A.; Sjoberg, B. *J. Am. Chem. Soc.* **1989**, *111*, 8087.
(31) Hurst, G.; Kraft, K.; Schultz, R.; Kreilick, R. *J. Magn. Reson.* **1982**, *49*, 159.
(32) Ruthroff, C. L. *Proc. IRE* **1959**, *August*, 1337.

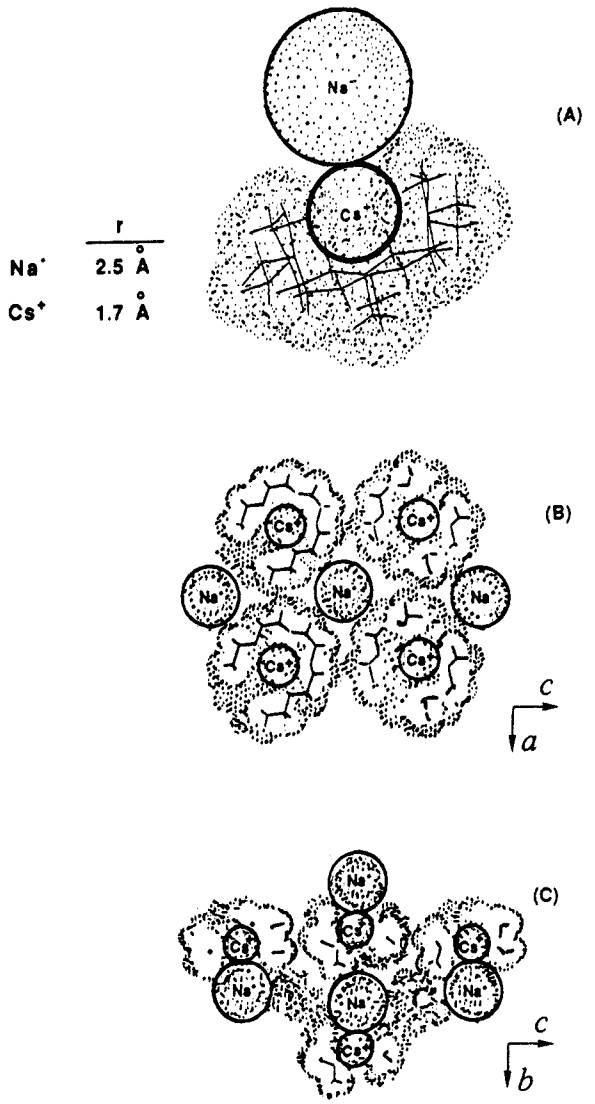

Figure 2. Computer simulation of the cation–anion packing in $Cs^+(HMHCY)\cdot Na^-$ from X-ray data: (A) the molecular unit, (B) cutaway view down the *b* axis, and (C) cutaway view down the *a* axis.

A computer simulation of the major octet of the EPR spectrum is shown in Figure 1B. This uses $g_\perp = 1.977$, $g_\parallel = 1.996$, and $A_\perp = 0.00937$ T, $A_\parallel = 0.01063$ T. The isotropic coupling constant, A_{iso}, of 0.00979 T corresponds to 11.9% atomic character, i.e., an electron density of 3.15×10^{30} e/m^3 at the cesium nucleus as a result of direct coupling of the electron to the cesium nucleus. The magnitude of the coupling to cesium is comparable to that of cesium–ethylamine solutions.[33]

The absence of substantial direct coupling to protons is not surprising. Solvated electrons in liquid ammonia[34] and trapped electrons in frozen alkali-metal–HMPA[35] and liquid crown ether solutions[36] show direct coupling to the alkali-metal nucleus but only weak coupling to the protons. In fact, a negative spin density, caused by spin polarization, has been observed by NMR for the proton in alkali-metal–ammonia solutions[34] while positive electron spin density occurs for the alkali-metal nucleus and the nitrogens of the solvent.[37]

2. The Crystallographic Structure. The nature of the electron-trapping site can be understood by reference to the crystal structure. $Cs^+(HMHCY)\cdot Na^-$ crystallizes[27,38] in the orthorhombic primitive system in the space group $P2_12_12_1$ with $a = 11.021$ (4) Å, $b = 11.13$ (4) Å, $c = 22.886$ (8) Å, and $Z = 4$. It can be viewed as a greatly distorted octahedral arrangement with a nearest cation–anion distance of 4.26 Å for a single cation–anion pair and remaining neighboring ions at distances ranging from 7.23 to 8.63 Å. Figure 2A is based on a computer-generated structure of the ion pair $Cs^+(HMHCY)\cdot Na^-$, obtained from the X-ray diffraction data. In each unit, the HMHCY ring has the four nitrogen atoms 4, 7, 13, and 16 in a plane while nitrogens 1 and 10 are below the plane by 1.43 and 1.14 Å, respectively. The corresponding four methyl groups attached to the planar nitrogen atoms are above the plane and form a rim around the "basket" while the other two methyl groups are below the plane, effectively closing the bottom of the "basket". The cesium cation is at the center of the cage, 0.9 Å above the plane of the four nitrogens, and forms a contact ion pair with the sodide anions. Parts B and C of Figure 2 show two cutaway views along the *b* and *a* axes, respectively, of the cation–anion packing in $Cs^+(HMHCY)\cdot Na^-$. The molecular units are ordered in a slightly staggered arrangement in such a way that each sodide ion is in close contact with one neighboring cesium cation. Otherwise, the sodium anion is effectively embedded in a "sea" of protons from the $-CH_3$ and $-CH_2-$ groups of the surrounding complexant molecules. The cation–anion packing does not allow the formation of other large natural cavities and therefore, the anionic sites are well-defined.

Table I. Sodium-to-Proton and Cesium-to-Proton Distances in $Cs^+(HMHCY)\cdot Na^-$ (within 5.0 Å)

Na^- to H distances, Å		Cs^+ to H distances, Å	
$-CH_3$ protons	$-CH_2-$ protons	$-CH_3$ protons	$-CH_2-$ protons
3.928	3.547	3.251	3.753
4.034	3.870	3.288	3.797
4.138	3.981	3.430	4.028
4.276	4.184	3.434	4.060
4.355	4.216	3.438	4.151
4.370	4.252	3.440	4.230
4.417	4.262	3.465	4.234
4.719	4.425	3.577	4.236
4.772	4.427	3.615	4.326
4.833	4.439	3.640	4.352
4.836	4.511	4.376	4.371
4.860	4.511	4.384	4.376
4.968	4.575	4.406	4.816
4.982	4.631	4.501	4.824
	4.633	4.551	4.825
	4.896	4.660	4.828
		4.984	4.834
			4.835
			4.846
			4.867
			4.873
			4.873
			4.878
			4.911

The crystal structure permits calculation of the sodium–proton and cesium–proton distances. These are shown in Table I separated into distances to methyl and methylene protons. An intriguing feature of $Cs^+(HMHCY)\cdot Na^-$ is that the optical and NMR spectra indicate the presence of Cs^+ and Na^- with very little charge transfer, in spite of the close contact between the cation and anion. This reflects the importance of cation complexation and its resistance to neutralization by electron transfer from the sodide anion or by covalent bond formation.

3. ^{1}H ENDOR. The ^{1}H ENDOR spectrum in the weak coupling region for the polycrystalline sodide $Cs^+(HMHCY)\cdot Na^-$ is shown in Figure 3B. Both this and the accompanying spectrum of the perdeuteriomethyl sodide (Figure 3C) were obtained at 120 K, a temperature at which we assume that the spectrum is simplified by motional averaging of the $-CH_3$ protons. This assumption is based upon additional data (not shown) that indicate

(33) Dye, J. L.; Dalton, L. R. *J. Phys. Chem.* **1967**, *71*, 184.
(34) Hughes, T. R., Jr. *J. Chem. Phys.* **1963**, *38*, 202.
(35) Catterall, R.; Edwards, P. P. *Adv. Mol. Relax. Interact. Processes* **1978**, *13*, 123.
(36) Holte, D. M.; Ellaboudy, A. S.; Edmonds, R. N.; Edwards, P. P. *Proc. R. Soc.* **1987**, *A415*, 212.
(37) Acrivos, J. Y.; Pitzer, K. S. *J. Phys. Chem.* **1962**, *66*, 1693.
(38) Kuchenmeister, M. E. Ph.D. Dissertation, Michigan State University, East Lansing, MI, 1989.

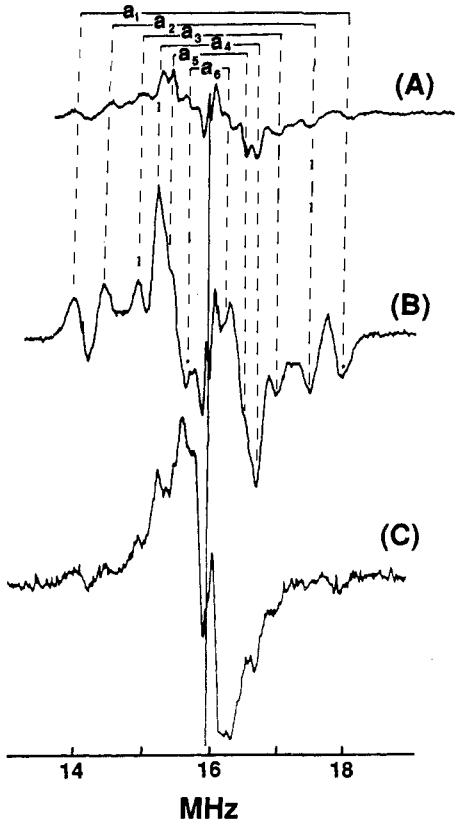

Figure 3. ^{1}H ENDOR spectra of polycrystalline Cs$^+$(HMHCY)·Na$^-$ at (A) 4 K and (B) 120 K and of perdeuteriomethyl Cs$^+$(HMHCY)·Na$^-$ at 120 K (C). The vertical line indicates the proton Larmor frequency at the magnetic field used to record these spectra.

no further line narrowing as the temperature is raised to 200 K. Upon cooling to 4 K, most of the lines remain but their relative amplitudes are altered (Figure 3A). These spectra were obtained by saturating the most intense EPR line shown in Figure 1A.

Specific deuteration of the methyl groups attached to the nitrogen atoms of the macrocycle provide a distinction of spectral contributions of the methyl group protons from those of protons bound directly to the carbons of the macrocyclic ring. Comparison of spectra B and C of Figure 3 indicates that electron-to-methyl proton interactions account for most of the ^{1}H ENDOR spectrum. Following deuteration of the methyl groups, only narrow lines near the proton Larmor frequency (here 15.9 MHz) are prominent. This indicates that either the protons of the macrocycle ring interact only very weakly with the trapped electron or the proton ENDOR signal is intrinsically weak for the $-CH_2-$ protons.

The EPR signal originates from a trapped electron that interacts strongly with one cesium nucleus. No strong ENDOR couplings were observed at high frequencies (i.e., up to 70 MHz). All proton ENDOR couplings were observed in the so-called "close coupling" region ($A \leq 5$ MHz) and, as such, are relatively weak.

At both 4 and 120 K, four signals on either side of the center of the ^{1}H ENDOR pattern can be unequivocally assigned to methyl protons. These are designated a_1 to a_4 in Figure 3. In addition, peaks separated by a_5 and a_6 and a shoulder between a_2 and a_3 can be identified, but these cannot be reliably separated from contributions of the methylene protons.

If the electron–proton interactions were purely dipolar with no Fermi contact contributions, we would observe *pairs* of lines that correspond to parallel and perpendicular components with $A_\parallel = 2|A_\perp|$. The parallel components would be positive to the left of the center frequency and negative to the right, while the perpendicular components would have both positive and negative contributions to the derivative spectra on both sides of the center. Unfortunately, it is not possible to simulate quantitative ENDOR spectra because of the complex relationships between intensities and relaxation times. Therefore, we cannot cleanly separate the effects of contact contributions from those due to dipolar interactions. However, the pronounced dip of the first peak below the baseline and the rise above the baseline of the corresponding peak on the right indicate that at least the signals designated by a_1 result from contact density at one or more of the methyl protons.

Table II. Hyperfine Tensor Components and Percent Atomic Character for Trapped Electrons in Cs$^+$(HMHCY)·Na$^-$

nucleus[a]	$A_\perp$, MHz	$A_\parallel$, MHz	r, Å	% atomic character[b]	
H_1	2.03 (a_3)	4.01 (a_1)	3.4	0.13	0.26
H_2	1.44 (a_4)	3.01 (a_2)	3.8	0.09	0.20
H_3	1.26[c]	2.51[c]	4.0	0.08[c]	0.18[c]
H_4	0.52 (a_6)	1.05 (a_5)	5.7	0.04	0.07
Na	+0.70[d]			0.079[d]	
	−0.80			0.091	
Cs_1	260	295		11.9	
Cs_2	+0.31[d]			0.014[d]	
	−0.41			0.018	

[a] Designation for hydrogen is to four groups of $-CH_3$ protons if dipolar coupling is assumed. [b] If the ENDOR peaks were due only to Fermi contact interactions these contact densities would be required. [c] From shoulders not indexed in Figure 3. The smaller of these two couplings is inferred from the peak shape. [d] Isotropic coupling constant. Different magnitudes are required to simulate the line shape for positive and negative coupling constants.

In the close coupling region, ENDOR transitions occur at frequencies $\nu_\pm = \nu_n \pm A/2$, where ν_n is the nuclear Larmor frequency and A is the appropriate hyperfine tensor component. Because of the inability to separate dipolar from contact contributions, the values a_1, a_2, ... were measured from peaks (or shoulders) on the left to valleys on the right, even though this is only appropriate for dipolar contributions.

It is possible to group the couplings pairwise to meet the criterion required for the dipolar case. This is done in Table II, and the calculated electron–proton distances (see Discussion) are included as if all peaks were the result of dipolar couplings. Table II also includes the percent atomic character that would be inferred if all of the peaks were the result of Fermi contact. The latter values have been corrected for the decreases in a_1, a_2, ... that would be required to represent the centers of the derivative signals in Figure 3B rather than the peak-to-valley distances.

The same coupling constants were found from the ENDOR spectrum at 4 K and also from the ^{1}H NMR ENDOR pattern obtained by saturating the central EPR transition of Figure 1A (data not shown). In the latter experiments the central ^{1}H frequency shifted as expected.

4. ^{23}Na and ^{133}Cs ENDOR. At a magnetic field of 0.373 T, sodium and cesium nuclei resonate at 4.20 and 2.10 MHz, respectively. The ^{23}Na and ^{133}Cs powder ENDOR spectra of trapped electrons in Cs$^+$(HMHCY)·Na$^-$ are shown in Figure 4A. The presence of a very sharp sodium ENDOR band in the frequency range of 3.5–5.0 MHz and the somewhat broader ^{133}Cs band between 1.75 and 2.60 MHz is clear.

A similar ^{23}Na ENDOR pattern was observed for Rb$^+$-(HMHCY)·Na$^-$ while the signal we attribute to ^{133}Cs ENDOR was absent. No ENDOR signal due to ^{87}Rb was seen. The rather weak hyperfine coupling observed for ^{133}Cs shows that it is due to a "distant" cesium nucleus (Cs_2) rather than the cesium nucleus (Cs_1) that is responsible for the observed powder EPR spectrum. The direct coupling of the electron to Cs_1 of 274 MHz that we have determined from the EPR spectrum (see above) is expected to produce an ENDOR pair centered at 137 MHz and separated by 4.2 MHz. These signals are well beyond the experimental frequency limit of our instrumentation. The structure observed in the ENDOR spectrum below 1.75 MHz in Figure 4A might be due to coupling to the nitrogen nuclei (ν = 1.14 MHz).

The ^{23}Na ENDOR pattern was also obtained by saturating the central EPR transition. The frequency shift was as expected for the lower field, the coupling frequency was unchanged, and the

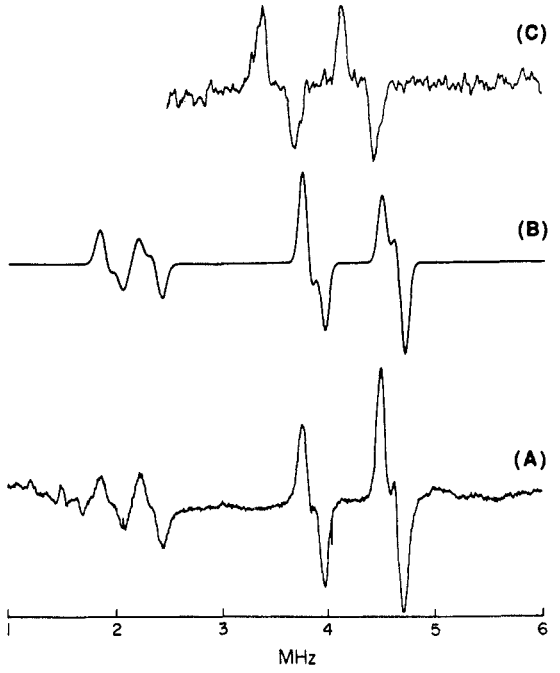

Figure 4. ^{23}Na (4.2 MHz) and ^{133}Cs (2.1 MHz) ENDOR spectra of polycrystalline $Cs^+(HMHCY)\cdot Na^-$ at 120 K. (A) The observed ENDOR spectrum at a field of 0.3727 T (indicated by the solid arrow in Figure 1). (B) The two NMR powder patterns simulated for each nucleus at a field of 0.3727 T. This simulation used positive hyperfine coupling constants. (C) The observed ^{23}Na ENDOR spectrum at a field of 0.3520 T (indicated by the dotted arrow in Figure 1).

individual lines were broadened (see Discussion).

Discussion

The EPR and ENDOR results presented here can be combined with structural data to obtain information about the nature of electron trapping in alkalide salts that contain the $M^+\cdot M^-$ ion pair. The simplest assumption is that electron trapping takes place in or near the anionic vacancies. This is appropriate for the case of $Cs^+(HMHCY)\cdot Na^-$ since the EPR spectrum shows that the electronic wave function overlaps strongly with the cesium s orbitals, and the X-ray structural data show the formation of a contact ion pair ($Cs^+\cdot Na^-$) when the anionic cavity contains the sodide ion. In addition, the sodide ions are well-isolated from each other. Thus, we propose an F-center model, with the center of the trapped electron density somewhere within the sodium anion site. In this case, the excess electron wave function interacts with several shells of surrounding matrix nuclei so many ENDOR lines are possible. Of course, the electron density may be displaced toward the Cs^+ cation as has been proposed[39] for the "monomer" species in metal–amine solutions. Because one face of the complexant is open, there is no barrier to electron overlap with Cs^+ as there is, for example, when sandwich complexes such as $Cs^+(18\text{-crown-}6)_2$ or cryptated complexes such as Cs^+(cryptand [2.2.2]) are formed.[40] Electrons trapped in alkalides with these cations show no evidence of hyperfine coupling to a single cesium cation.

The anisotropy of the EPR spectrum shown in Figure 1 as well as the low g value provides direct evidence that the $Cs^+\cdot e^-$ system is not spherical. The simplest explanation is strong interaction between the complexed cesium cation and the trapped electron, giving considerable 6s character to the trapped electron wave function but not as much as in the free cesium atom. The trapped electron has 11.9% atomic character, a value that is similar to that of cesium in ethylamine at room temperature.[33]

Geometric information can be obtained from ENDOR frequencies when the anisotropic hyperfine coupling arises from through-space electron–nuclear dipolar interaction between a localized electron spin and nearby nuclei. At the high-field limit, i.e., when the coupling is weak enough to be treated as a minor perturbation, the classical approximation for the interaction between the point-dipole electron spin and the nucleus may be used[41–43] to calculate the dipolar hyperfine coupling components as

$$A_\perp = \frac{-g_e\beta_e g_n\beta_n}{r^3};\ A_\parallel = 2|A_\perp| \qquad (2)$$

where r is the distance between the localized electron and the nucleus in question, g_n is the nuclear g factor, β_e and β_n are the electron and nuclear Bohr magnetons, respectively, and g_e is the effective electronic g value.

The effective electron nuclear distances obtained by using the couplings obtained from a_1–a_4 of Figure 3 are 3.4 and 3.8 Å, respectively. Less-well-defined couplings correspond to distances of 4.0 and 5.7 Å. It should be noted that the signal used to obtain the distance of 3.4 Å probably results from contact interactions so that this distance is not meaningful.

The effective distances from the electron to $-CH_3$ protons are comparable to the Na^- to H and Cs^+ to H distances given in Table I. Exact correspondence is not anticipated because of the use of the point-dipole approximation and the neglect of contact interaction, assumptions that are certainly not valid for the diffuse electron density expected for a trapped electron. If the form of the trapped electron wave function were known, one could use a distributed charge model to calculate the dipolar coupling as carried out for π-electron radicals by McConnell and Strathdee.[44] We have also used the distributed charge approach previously to calculate dipolar couplings in various aromatic free radicals.[30,42]

In the present case, a hydrogenic wave function for the trapped electron

$$\psi_e = \pi^{-1/2}a_0^{-3/2}e^{-r/a_0} \qquad (3)$$

leads to the hyperfine coupling component

$$A_\parallel = 2g_e\beta_e g_n\beta_n/R^3$$

in which R is the distance between the center of the trap and the nucleus in question and $a = R/a_0$. For large values of a this reduces to the point-dipole expression. The second term in eq 4 serves to decrease the coupling relative to the point-dipole approximation, leading to even smaller values of R than those given in Table II.

The distances calculated with the assumption that the ^1H ENDOR pattern is the result of dipolar coupling between the trapped electron and the protons are reasonable, especially if the largest couplings are assigned to contact interactions. The large effect of substituting $-CD_3$ for $-CH_3$ is, however, puzzling, since the $-CH_3$ and $-CH_2-$ protons are at comparable distances from any reasonable trapping site. Of course, the ENDOR sensitivities to the two types of protons could be very different, but it seems equally reasonable that the contact densities might be very different for methyl and methylene protons.

To compare the expected ENDOR dipolar pattern from $-CH_3$ and $-CH_2-$ protons, the distances given in Table I were used to compute the two patterns, assuming intrinsically equal sensitivities for all protons. The patterns were remarkably similar and quite insensitive to the location of the center of unpaired electron density. This reinforces the idea that both contact and dipolar interactions are important.

If the peaks in the proton ENDOR spectra arise from Fermi contact interactions, the spin densities at protons can be calculated from the positions of the peaks. The calculated hydrogen atomic character varies from 0.26 to 0.04% of that of a gaseous hydrogen atom, which has an A value of 0.0507 T (1420 MHz).[45]

(39) Dye, J. L. *Pure Appl. Chem.* **1977**, *49*, 3.
(40) Shin, D.-H.; DeBacker, M. E.; Ellaboudy, A. S.; Dye, J. L. Unpublished results.
(41) Wertz, J. E.; Bolton, J. R. *Electron Spin Resonance. Elementary Theory and Practical Applications*: McGraw-Hill: New York, 1972.
(42) O'Malley, P. J.; Babcock, G. T. *J. Am. Chem. Soc.* **1986**, *108*, 3995.
(43) Wells, G. B.; Makinen, M. W. *J. Am. Chem. Soc.* **1988**, *110*, 6343.
(44) McConnell, H. M.; Strathdee, J. *Mol. Phys.* **1959**, *2*, 129.
(45) Wittke, J. P.; Dicke, R. H. *Phys. Rev.* **1956**, *103*, 620.

It is clear that the ^1H ENDOR pattern of electrons trapped in Cs^+(HMHCY) results from a combination of dipolar and contact hyperfine interactions. The contact densities required are small and the dipolar contributions are consistent with the distances to protons from the center of the anionic trapping site. These results and the pronounced hyperfine coupling to one cesium ion are consistent with an F-center model in which the electron is trapped at an anion vacancy but is probably polarized toward the unique cesium cation that is in contact with Na^- when the cavity is occupied by this ion. It remains to be shown that this picture is consistent with the ^{133}Cs and ^{23}Na ENDOR patterns.

The sodium and cesium ENDOR spectra arise from the same electrons that yield the cesium hyperfine pattern and the coupling to methyl protons. The reason is that these ENDOR patterns were obtained with the EPR spectrometer tuned to one of the cesium hyperfine lines, so the *same* trapped electron that interacts strongly with a single cesium nucleus also gives the weaker coupling to the more distant Na^- and Cs^+ ions. The observed EPR spectrum, particularly its homogeneous power saturation behavior, also rules out a broad distribution of trapping sites for the electron.

If the ^{23}Na and ^{133}Cs ENDOR patterns were due to dipolar coupling with the trapped electron they would imply distances of 3.5 and 3.9 Å, respectively. These values are far too small to be consistent with the structure, since the nearest Na^- and Cs^+ ions to the trapping center are of the order of 8 Å away. In addition, the pattern does not show the clean signals expected for $A_\parallel$ and $A_\perp$ at frequencies that differ by a factor of 2. The absence of an ^{87}Rb ENDOR signal from Rb^+(HMHCY)·Na^- suggests that the Cs and Na ENDOR spectra result from quadrupolar interactions rather than dipolar interactions. Simulation of the ^{87}Rb NMR spectrum of Rb^+(HMHCY)·Na^- at a field of 9.7 T yields a quadrupole coupling constant (QCC) of 13 MHz[46] which would broaden an ENDOR line beyond detection. The alternative to a purely dipolar interaction is Fermi contact density of the trapped electron at the sodium and cesium nuclei caused by the "tail" of the electron density distribution. This would lead to two NMR powder patterns, one on either side of the NMR frequency. Derivative line shapes were calculated by adjusting the quadrupole coupling constant and the Gaussian dipolar contribution (from surrounding atoms). The simulations are shown in Figure 4B along with the experimental ENDOR patterns. The hyperfine coupling to ^{23}Na corresponds to +0.70 MHz or 0.079% atomic character, while that to ^{133}Cs is +0.31 MHz or +0.014% atomic character assuming positive A values. The line shapes correspond to quadrupole coupling constants of 2.3 MHz for Na^- and 5.3 MHz for Cs^+. These values of QCC are larger than those typical of isolated Na^- and Cs^+ and probably reflect the large field gradient in the ion pair. Gaussian half-widths of 86 and 96 kHz for Na^- and Cs^+ compare with calculated dipolar contributions of 67 andf 53 kHz, respectively, obtained by using the Van Vleck equation.[47]

Confirmation of the quadrupolar nature of the ^{23}Na ENDOR pattern was obtained from the signal that resulted from saturation of a central line of the EPR pattern as shown in Figure 1. At this lower field, the center of the pattern shifted from 4.20 to 3.9 MHz as expected. Furthermore, the hyperfine coupling constant was unchanged, but the line width of the second-order quadrupolar powder pattern increased by 5%, within experimental error of that expected for the 7% decrease in the external field. This experiment provides clear evidence for a contact hyperfine interaction with Na^- and the resulting quadrupolar powder pattern.

From the static and MAS NMR spectra for ^{133}Cs and ^{23}Na in polycrystalline Cs^+(HMHCY)·Na^- we estimate quadrupole coupling constants of ~2 and ~6 MHz for Na^- and Cs^+, respectively, in reasonable agreement with those required to simulate the ENDOR spectra. It is likely that the QCC values near a defect electron site may be different than those in the pure sodide.

The program VMASS,[48] which is based on the high-field approximation, was used to simulate Na and Cs ENDOR powder patterns. Since the quadrupolar frequencies are large, the validity of the high-field approximation deserves comment. Lamarche et al.[49] calculated NMR transition frequencies of Al with a quadrupole coupling constant of 2.9 MHz as a function of external field strength. Their results showed that 5 satellite transitions corresponding to the high-field case were obtained at a field of only 0.1 T or above. The Larmor frequency for Al at this field is 1.11 MHz and the quadrupolar frequency (ν_Q) is 0.444 MHz. The ratios, ν_Q/ν_n, for Na^- and Cs^+ are 0.27 and 0.18, respectively, even smaller than that of Al under conditions that permit use of the high-field approximation.

The contact densities at Na^- and Cs^+ are comparable to those at Cs^+ in Cs^+(18-crown-6)$_2$·e^-[50] and Cs^+(15-crown-5)$_2$·e^-[51]) in which the electron wavefunction is presumed to be centered at the anionic vacancies with only weak overlap with the sandwiched cesium cation. The larger contact density at Na^- than at Cs^+ may reflect the fact that the electron wavefunction can overlap with Na^- through a weak barrier as shown in Figure 2B. The data do not provide information about the number of "distant" Na^- and Cs^+ ions involved. From the structure shown in Figure 2 we can assign probable upper limits of 6 and 5, respectively, but the asymmetry is such that fewer interactions could dominate. The contact density at the unique Cs^+ is large, but it is still too small to correspond to trapped atoms. This is in contrast to the behavior of solvated hydrogen and silver atoms in frozen solutions[52,53] or in alkali halide crystals,[54] which show 88–99% atomic character.

In conclusion, combined EPR, ENDOR, and structural data have been used to probe the local structure of trapped electrons in alkalide salts. F-center trapping at an anion vacancy accounts well for all of the results, but the extent to which the electron density is polarized toward Cs^+ cannot be obtained from the data.

Acknowledgment. This research was supported by the U.S. National Science Foundation Solid State Chemistry Grant No. DMR 87-14751, by NATO Grant No. 0106/89, and by NIH Grant GM 37300. EPR analysis software was furnished by the Illinois EPR Research Center, NIH Division of Research Resources Grant No. RR01811. We are also grateful to Professor Marc DeBacker of the Laboratoire de Chimie Physique, Lille, France, for early studies of the EPR spectra of Cs^+-(HMHCY)·Na^-.

(46) Kim, J.; Eglin, J. L.; McMills, L. E. H.; Ellaboudy, A. S.; Dye, J. L. Unpublished results.
(47) Van Vleck, J. H. *Phys. Rev.* **1948**, *74*, 1168.
(48) Kim, J.; Dye, J. L.; Story, H. S.; Kline, D. Quantum Chemistry Program Exchange, QCMP 056; Indiana University: Bloomington, Indiana.
(49) Lamarche, G.; Volkoff, G. M. *Can. J. Phys.* **1953**, *31*, 1011.
(50) Dawes, S. B.; Ellaboudy, A. S.; Dye, J. L. *J. Am. Chem. Soc.* **1987**, *109*, 3508.
(51) Dawes, S. B.; Eglin, J. L.; Moeggenborg, K. J.; Kim, J.; Dye, J. L. Unpublished results.
(52) Shields, L.; Symons, M. C. R. *Mol Phys.* **1966**, *11*, 57.
(53) Shields, L. *J. Chem. Phys.* **1966**, *44*, 1685.
(54) Delbecq, C. J.; Hayes, W.; O'Brien, M. C. M.; Yuster, P. H. *Proc. R. Soc.* **1963**, *A271*, 243.